PCCP

Accepted Manuscript

ROYAL SOCIETY OF CHEMISTRY

www.rsc.org/pccp

Are intramolecular frustrated Lewis pairs also intramolecular catalysts? A theoretical study on H_2 activation.

Lei Liu Zeonjuk,[a] Petko St. Petkov,[a] Thomas Heine,[a] Gerd-Volker Röschenthaler,[a] Johannes Eicher,[b] Nina Vankova,[*a]

[a]Department of Physics & Earth Sciences, Jacobs University Bremen, Campus Ring 1, 28759 Bremen, Germany

[b]Solvay Fluor GmbH, Hans-Böckler-Allee 20, 30173 Hannover, Germany

Abstract

We investigate computationally a series of *intramolecular* frustrated Lewis pairs (FLPs), with the general formula $Mes_2PCHRCH_2B(C_6F_5)_2$, that are known from the literature to either activate molecular hydrogen (FLPs with R = H (**1**) or Me (**4**)), or remain inert (FLPs with R = Ph (**2**) or $SiMe_3$ (**3**)). The prototypical system $Mes_2PCH_2CH_2B(C_6F_5)_2$ (**1**) has been described in the literature (Grimme et al., *Angew. Chem. Int. Ed.* **2010**; Rokob et al., *J. Am. Chem. Soc.* **2013**) as an *intramolecular* reactant that triggers the reaction with H_2 in a bimolecular concerted fashion. In the current study, we show that the concept of *intramolecular* H_2 activation by linked FLPs is not able to explain the inertness of the derivative compounds **2** and **3** towards H_2. To cope with this, we propose an alternative *intermolecular* mechanism for the investigated reaction, assuming stacking of two open-chain FLP conformers, and formation of a dimeric reactant with two Lewis acid-base domains, that can split up to two hydrogen molecules. Using quantum-chemical methods, we compute the reaction profiles describing these alternative mechanisms, and compare the derived predictions with earlier reported experimental results. We show that only the concept of *intermolecular* H_2 activation could explain both the activity of the FLPs having small substituents in the bridging molecular region, and the inertness of the FLPs with a bulkier substitution, in a consistent way. Importantly, the *intermolecular* H_2 activation driven by *intramolecular* FLPs indicates the key role of steric factors and noncovalent interactions for the design of metal-free systems that can efficiently split H_2, and possibly serve as metal-free hydrogenation catalysts.

Keywords: metal-free catalysis, hydrogen activation; frustrated Lewis pairs; reaction mechanism; density functional theory; *ab initio* calculations

Introduction

Activation of molecular hydrogen is a subject of substantial research interest due to the key role of H_2 in the chemical and petrochemical industries, and as a source of clean and renewable energy. Particularly desirable, in view of reducing costs and environmental issues, yet rather challenging, is the design of transition metal (TM)-free catalysts capable of activating H_2 at mild conditions. A major breakthrough in this direction was achieved less than a decade ago with the discovery of sterically hindered TM-free Lewis acid-base pairs that can split heterolytically the H–H bond, in a reversible or irreversible manner, and thus, find application as catalysts in various hydrogenation reactions. Such *intra*- or *intermolecular* Lewis acid-base combinations with bulky substituents at the active sites, capable of activating small molecules, such as H_2, CO_2, alkenes, etc., are known as frustrated Lewis pairs (FLPs), and since the first prototypical examples reported by the Stephan group,[1,2] a variety of FLPs with P, N or C as the donor, and B or Al as the acceptor site has appeared in the literature.[3–6] The rapid accumulation of experimental data in the field has entailed a number of computational studies employing density functional theory (DFT) and *ab initio* static calculations, as well as molecular dynamics simulations for rationalizing the actual mechanism of the underlying processes, and the key factors determining the FLPs' activity.[7–13]

An interesting early example of an *intramolecular* (linked) FLP that rapidly activates H_2 at room temperature is the ethylene-bridged phosphane-borane adduct $Mes_2PCH_2CH_2B(C_6F_5)_2$ (**1**, Table 1) reported by Spies et al.[2] Adduct **1** has been characterized by means of ^{1}H, ^{19}F, ^{11}B and ^{31}P NMR spectroscopic studies and DFT calculations to exhibit a four-member heterocyclic structure with a substantial P–B donor-acceptor interaction, and calculated P–B distance of only 2.21 Å) (Table 1). Additionally, the DFT results have indicated that this unusual heterocycle is stabilized by noncovalent interactions (π-stacking) between the spatially close aryl substituents at phosphorus and boron. Besides the global minimum cyclic structure of compound **1**, two isoenergetic open-chain local minima with *gauche* and *trans* conformations have been localized by the DFT studies. These noncyclic conformers have been predicted to lie *ca.* 29.3 kJ·mol^{-1} above the cyclic ground state (B97D/def2-TZVP gas-phase calculations), and assumed to be responsible for the observed heterolytic cleavage of H_2.[2] The mechanism of this process has been further explored by means of DFT and SCS-MP2 methods, and as a result, the H_2 activation has been rationalized as a bimolecular concerted reaction between the *gauche* conformer of FLP**1** and the hydrogen molecule.[10,12] Within the model proposed firstly by Grimme et al.,[10] the key step in the whole process is the entrance of the H_2 molecule into the *intramolecular* reactive pocket framed by the P and B sites in *gauche*-**1**. In the structure of the located transition state (TS), FLP**1** retains the *gauche* conformation, and H_2 lies away from the P···B axis. Due to the electric field created by the closely lying Lewis sites, the entrapped H_2 becomes polarized, and eventually, splits to a proton and a hydride attached to the phosphorus and boron, respectively, in the hydrogenated product. Later, Pápai and co-workers have studied the same process of *intramolecular* activation of H_2 by FLP**1**, and, differently from the electric field based explanation of Grimme et al.,[10] have highlighted as a key element in the TS

nature, the FLP/H_2 orbital interactions enabling synchronous electron transfer from the lone pair of the donor to the empty orbital of the acceptor site, across the H···H bridging unit.[12] Despite this qualitative difference, the TS for the cleavage of H_2 in the presence of FLP**1**, as found by Rokob et al.,[12] is structurally rather similar to the earlier reported TS of Grimme et al.[10] It has a *gauche* conformation, and would eventually relax to the *gauche* conformer of the hydrogenated product. However, only *trans* conformers have been observed in the reported[2] crystal structure of the phosphonium–hydridoborate zwitterion, $Mes_2PH^+CH_2CH_2BH^-(C_6F_5)_2$, isolated at the end of the reaction. At this point, we should note that the *intramolecular* mechanism for the reaction between **1** and H_2, as proposed by Grimme et al.[10] and Rokob et al.,[12] has been discussed with emphasis on the nature and properties of the associated transition state, while the product side of the reaction coordinate, and in particular, the relative stability and interconversion of the *gauche* and *trans* hydrogenated products, has not been studied in detail. In principle, the experimental fact that only *trans* conformers of the zwitterionic salt of **1** are obtained at the end of the reaction can be rationalized in two different ways: (i) The hydrogenated *gauche* conformer obtained from the *intramolecular* TS is thermodynamically less stable than the *trans* conformer, and the latter is formed as a result of a facile and rapid *gauche-trans* isomerization (Scheme 1), or (ii) The H_2 activation occurs via a different reaction channel that avoids the formation of *gauche* intermediates, and yields directly the hydrogenated *trans* product. For achieving this, the *gauche-trans* isomerization has to take place prior the reaction with H_2, and, as a next step, close stacking of *trans*-**1** conformers into a dimer-like assemblies, resembling *intermolecular* FLPs, occurs as a result of non-covalent interactions, and causes the reaction with H_2 (Scheme 2). This second hypothesis describes an *intermolecular* reaction channel, and has not been considered so far in the literature for interpreting the reactivity of FLP**1** with H_2. Yet, it has been explored by Guo and Li for understanding the H_2 activation by the prototypical *intramolecular* FLP, $Mes_2P(C_6F_4)B(C_6F_5)_2$,[1] and has been qualified by them as the more favorable mechanism, in comparison to the other two alternatives for this system: the proton transfer and the hydride transfer mechanisms.[7]

Herein, we reinvestigate the mechanism of H_2 activation by *intramolecular* (linked) FLPs, considering the ethylene-bridged prototypical example $Mes_2PCH_2CH_2B(C_6F_5)_2$ (**1**), and a series of substituted derivatives of **1**, $Mes_2PCHRCH_2B(C_6F_5)_2$, listed in Table 1. In these derivatives, one hydrogen from the ethylene bridge between the Lewis sites (P and B) is substituted by either a phenyl (**2**), trimethylsilyl (**3**), or methyl (**4**) group. This imposes additional steric hindrance, especially in the structures of the Ph– and $SiMe_3$–substituted compounds **2** and **3**. Alike the parent FLP**1**, the three derivatives have been experimentally characterized as exhibiting a four-member cyclic structure with a P–B bond, typical of classical Lewis adducts.[4] For all of them, a facile ring opening has been experimentally verified, yet, only FLP**4** has been found to successfully cleave H_2, whereas FLPs **2** and **3** have remained inactive.[4] Employing dispersion-corrected DFT, substantiated by SCS-MP2 energy calculations, we model the complete reaction profiles corresponding to the *intra*- and *intermolecular* concepts outlined above, and compare the derived predictions with the

reported experimental findings,[2,4] with the aim to determine the actual mechanism of the H_2 heterolytic splitting by FLP **1**, and to elucidate the yet not fully understood different reactivity of FLPs **2**-**4** towards molecular hydrogen. In the current study, the possibility for accomplishing *intermolecular* H_2 activation by such *intramolecular* alkylene-bridged frustrated Lewis pairs is considered for the first time. On the basis of the performed analysis, we question the literature established *intramolecular* concept, and show that the *intermolecular* alternative provides more reasonable and consistent explanation for both the activity of the alkylene-linked FLPs with small substituents in the bridging molecular region (R = H and Me), and the inertness of the FLPs with a bulkier substitution therein (R = Ph and $SiMe_3$).

Table 1. Investigated intramolecular phosphane-borane adducts of the type $Mes_2PCHRCH_2B(C_6F_5)_2$ (R = H, Ph, $SiMe_3$, Me), with experimentally examined reactivity towards H_2 activation.[2,4]

System notation	Investigated linked FLPs	Global minimum structure (*cis* conformer)	Experimental results
1	$Mes_2PCH_2CH_2B(C_6F_5)_2$	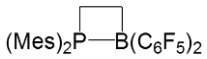	H_2 activation[2, a]
2	$Mes_2PCHPhCH_2B(C_6F_5)_2$	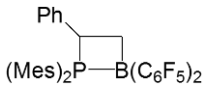	no reaction with H_2[4, b]
3	$Mes_2PCH_2CH(SiMe_3)B(C_6F_5)_2$	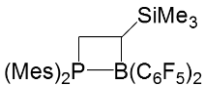	no reaction with H_2[4, b]
4	$Mes_2PCHMeCH_2B(C_6F_5)_2$	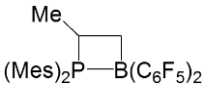	H_2 activation[4, c]

Reported experimental conditions: [a] 1.5 atm of H_2 pressure, in pentane; [b] 2.5 or 60 atm of H_2 pressure, in pentane or toluene, [c] 2.5 atm of H_2 pressure, in pentane.

Computational Details

Density Functional Theory (DFT) and *ab initio* calculations were carried out by using Gaussian09[14] and Turbomole 6.4[15] packages, respectively. Following our previously established computational protocol,[13] we employed the dispersion-corrected B97D exchange-correlation functional[16] with the 6-31G(d) double-ζ polarized basis set,[17,18] and the ultra-fine grid to optimize the geometries and calculate vibrational frequencies for all stationary points along the considered reaction coordinates. Gibbs energies were calculated via a harmonic analysis within the ideal-gas approximation. The absence of imaginary frequencies confirmed the local minimum character of all reactants and products, and the transition states (TS) were verified by the presence of one and only one imaginary frequency corresponding to atomic displacements in the P···H···H···B fragment. Intrinsic reaction coordinate (IRC) calculations were carried out for verifying the true connection between the reactants and the products.[19] Natural Population Analysis (NPA) was also performed using the Natural Bond Orbital[20] (NBO 3.1) program in Gaussian09. The solvent effect (toluene, ε = 2.3741) was accounted via single point calculations on the gas-phase optimized geometries employing the

polarizable continuum model (PCM).[21] Accurate electronic energies were derived by means of single point calculations at the spin-component-scaled second-order Møller-Plesset (SCS-MP2) level,[22] with the correlation-consistent triple-ζ polarized (cc-pVTZ) basis set,[23] and the resolution-of-identity (RI) integral approximation, as implemented in Turbomole 6.4.[24,25] Throughout the discussion (unless stated otherwise), we refer to SCS-MP2/cc-pVTZ-computed values of the potential energy at 0 K, coupled with B97D/6-31G(d)-derived zero-poit energy (ZPE), thermal and solvent corrections, as obtained for gas-phase optimized geometries.

To assess the dependence of the results on the computational level, we carried out a series of test calculations employing computationally more expensive XC functionals, basis sets, and solvent treatment for the three possible conformers of FLP **1** (**1**, *gauche*-**1** and *trans*-**1**), and for the stationary points characterizing the *intra*- and *intermolecular* mechanisms of H_2 activation. We probed the performance of the dispersion-corrected range-separated ωB97X-D functional[26] and the larger 6-31+G(d,p) basis set, augmented with diffuse functions and polarization on hydrogen atoms,[27–29] and we conducted geometry optimizations in PCM. In addition, we made test calculations using the D3-corrected GGA functional B97D3,[30] and the global hybrid Minnesota functional M062X,[31] to assess the quality of the dispersion-corrected energies. The values (ΔE and ΔG) derived at the explored theoretical levels are tabulated in the Supporting Information (Tables S1-S6). Though slightly different, they lead to essentially the same trends and conclusions about the energetics and the structure of the species characterizing the reaction profile.

As pointed out previously,[13] the adopted computational approach is not expected to provide very accurate Gibbs energies for direct comparison with the experimentally measured quantities, mainly due to the non-negligible errors which might be introduced from the use of the rigid-rotor harmonic approximation for computing the vibrational spectra of the weakly interacting systems studied here. Yet, this approach is adequate enough to provide qualitative trends, and is commonly applied for predicting FLP's thermochemistry and reaction kinetics.[9, 12, 13]

Results and Discussion

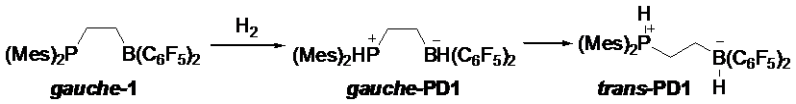

Scheme 1. Reaction of $Mes_2PCH_2CH_2B(C_6F_5)_2$ (**1**) with H_2, accomplished via an *intramolecular* mechanism, as proposed in Refs. [10] and [12].

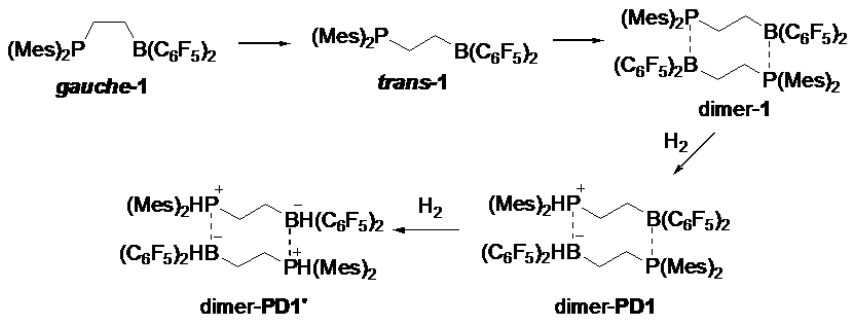

Scheme 2. Reaction of $Mes_2PCH_2CH_2B(C_6F_5)_2$ (**1**) with H_2, accomplished via an *intermolecular* mechanism, as proposed in the current work.

Our calculations yielded essentially the same global minimum structure of $Mes_2PCH_2CH_2B(C_6F_5)_2$ (**1** in Table 1) as the originally proposed by Spies et al.[4] As shown in Figure 1A, the four-member PCCB ring in **1** is stabilized by π–π stacking between one mesityl and one C_6F_5 substituent at phosphorus and boron, respectively, and the calculated P–B distance is rather short (d_{PB} = 2.25 Å), which is typical of a classical phosphane-borane adduct. The quenched acidity and basicity of the Lewis sites (B and P) in this adduct **1** renders it unable to react with H_2, and implies that other, more open, isomers are thermodynamically accessible and responsible for the observed H_2 activation. Similar to Grimme and co-wokers,[2] we also identify two local minima with open-chain structures: a *gauche* conformer with d_{PB} = 3.28 Å and PCCB torsion angle of 301º, and a *trans* conformer with d_{PB} = 4.04 Å and PCCB torsion angle of 145º (cf. *gauche*-**1** and *trans*-**1** in Figure 1A). However, in contrast to the previous findings that these two conformers are isoenergetic,[2] in our study, *trans*-**1** is found to be slightly more stable than *gauche*-**1**. The destabilization with respect to **1** amounts to about 24 kJ·mol^{-1} for *trans*-**1**, and 40 kJ·mol^{-1} for *gauche*-**1**, in terms of solvent-phase potential energy (ΔE_{sol}) at the SCS-MP2/cc-pVTZ//B97D/6-31G(d) level of theory. When entropy contributions are also accounted for, the destabilization (ΔG_{sol}) reduces to 15 kJ·mol^{-1} for *trans*-**1** and 29 kJ·mol^{-1} for *gauche*-**1**, while the energy difference between *trans*-**1** and *gauche*-**1** remains almost the same. Note that the relative energetics as predicted for the three conformational isomers of **1** follows the same trend, that is E(**1**) < E(*trans*-**1**) < E(*gauche*-**1**), independent of the used computational level (Table S1 in SI). The NPA-derived partial atomic charges clearly show that in adduct **1**, there is a considerable charge transfer between the closely lying Lewis sites that amounts to 0.74e shift of electron density from P to B, whereas in the case of the two non-cyclic *gauche*-**1** and *trans*-**1** conformers, such polarization does not occur (Table 2).

Similarly, for the phenyl-substituted derivative $Mes_2PCHPhCH_2B(C_6F_5)_2$ (**2** in Table 1), we identified three conformational isomers, see Figure 1B. Besides the global minimum cyclic structure, denoted as **2** (with d_{PB} of 2.17 Å, and PCCB torsion angle of 11º), our calculations yield two non-cyclic and isoenergetic local minima, which lie ~24 kJ·mol^{-1} above **2**, and correspond to a *cis*-**2** conformer (d_{PB} = 2.77 Å, PCCB = -19º), and a *trans*-**2** conformer (d_{PB} = 4.11 Å, PCCB = 149º).

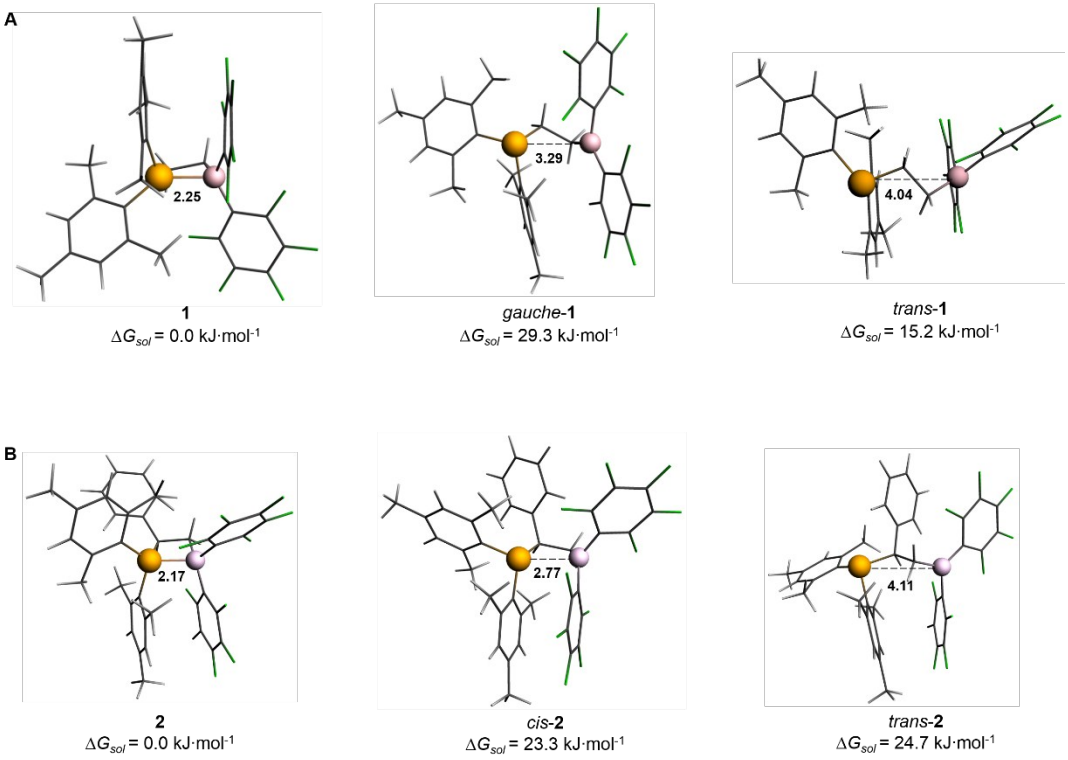

Figure 1. DFT predicted structures of the three conformers of $Mes_2PCH_2CH_2B(C_6F_5)_2$, FLP**1**, in (A), and $Mes_2PCHPhCH_2B(C_6F_5)_2$, FLP**2**, in (B), with the corresponding P–B distances, d_{PB}, in Å. The structures are derived at the B97D/6–31G(d) level (gas-phase calculations). The associated relative Gibbs energy values, ΔG_{sol}, are derived from solvent-corrected SCS-MP2/cc-pVTZ//B97D/6-31G(d) calculations. Color code: P yellow, B pink, F green, C grey, H white.

Importantly, the isomerization between the two open-chain minima of FLP**1** (*gauche*-**1** and *trans*-**1**) is predicted to be a rather facile process, with an estimated kinetic barrier of the order of 30 kJ·mol^{-1} relative to *gauche*-**1** (Figure S1).[32] As for FLP**2**, the ring opening process, as well as the rotational freedom around the PCCB axis, have been experimentally verified from the lineshape analysis of temperature-dependent dynamic ^{19}F NMR spectra.[4] Hence, the reaction with H_2 may be initialized by any of the two non-cyclic conformations of **1** and **2**, which in turn, opens up the possibility of having different reaction channels. If the initial (reactant) state is represented mainly by *gauche*-**1** of FLP**1** (and *cis*-**2** of FLP**2**), the reaction with H_2 can be described as a truly bimolecular process between one molecule of *gauche*-**1**, for FLP**1** (or one molecule of *cis*-**2**, for FLP**2**) and one hydrogen molecule (Scheme 1). This *intramolecular* reaction channel, as proposed in the literature to explain the reactivity of FLP**1**, has been only partially investigated, with emphasis on the nature and properties of the associated transition state (TS).[10,12]

On the other hand, if FLP**1** (or FLP**2**) is mostly in its *trans* conformation upon the attack of H_2, the reaction may proceed in a rather different way that involves, as a first step, stacking of two *trans*-**1** (or *trans*-**2**, for FLP**2**) molecules and formation of a dimer-like structure, resembling an *intermolecular* frustrated Lewis pair with two reactive pockets (Scheme 2). This alternative *intermolecular* reaction channel has not been explored so far for the series of ethylene-bridged FLPs

(**1**-**4**), and we consider it here for the first time. In the following, we present our findings for the possibilities of accomplishing an *intramolecular* or an *intermolecular* H_2 activation by FLPs**1** and **2**. For each reaction mechanism, we discuss all stationary points located along the corresponding reaction coordinate, and the associated energy barriers.

***Intramolecular* H_2 activation.** Figure 2A illustrates the reaction profile calculated in the case of *intramolecular* H_2 activation by FLP**1** (see also Scheme 1). The solvent–phase potential energies (ΔE_{sol}) and Gibbs energies (ΔG_{sol}) associated to the stationary points along the reaction path are shown relative to E_{sol} and G_{sol} characterizing the two reactants – *gauche*-**1** and a free hydrogen molecule. The energetics of the ring-like global minimum **1** is shown only for completeness (we have not studied the kinetics of the ring opening process). It is obvious from Figure 2A that the reaction between *gauche*-**1** and H_2 is an uphill process that requires overcoming an energy barrier of almost 100 kJ·mol^{-1} at room temperature (65 kJ·mol^{-1} at 0K). This energy cost is of the same order of magnitude as the one predicted (at the same level of theory) in our previous study[13] for the activation of H_2 by the weakly bound, *intermolecular* FLP combining similar components, namely, Mes_3P and $B(C_6F_5)_3$. The located transition state, TS**1a**, is characterized by a single imaginary frequency (f_i = -95 cm^{-1}) corresponding to the movement of H_2 towards the reactive pocket framed by phosphorus and boron, and to the stretching of the H–H bond. In TS**1a** (see Figure 3A for the structure), the distance between P and B increases by 0.08 Å compared to d_{PB} in the *gauche*-**1** reactant, and the entrapped hydrogen molecule is stretched by 0.09 Å with respect to the equilibrium H–H bond length (cf. the respective d_{HH} values in Table 2). The elongation of the H–H bond is accompanied by formation of partial P–H and B–H bonds (d_{PH} = 1.93 Å and d_{BH} = 1.55 Å) in a simultaneous fashion, as evidenced by the conducted IRC calculation. The elongated H_2 lies away from and slightly inclined to the P–B axis (with PHH and BHH angles of 153º and 120º, respectively), which is indicative for end-on P···H_2 and side-on B···H_2 interactions in TS**1a**. This feature has been found in previous studies for the same, as well as for other FLPs,[7,8,10,11,12,13] and has been highlighted as an important characteristics of the TS of a reactive FLP. Besides the structural changes, an important feature of TS**1a** is the electron density redistribution between the active sites of FLP**1** and the closely lying H_2, which differs considerably from the situation on the reactant side (*gauche*-**1** + H_2). The polarization of H_2 in TS**1a** amounts to 0.13e, as quantified by the difference between the natural charges of the H_2-end close to phosphorus (H_p) and the H_2-end close to boron (H_B). The donor and acceptor sites become also polarized, as indicated by the 0.34e shift of electron density from P to B (see Table 2). This charge transfer engaging the Lewis sites and the entrapped hydrogen molecule in TS**1a** preconditions the heterolytic splitting of the H–H bond in the subsequent reaction step. The relaxation of TS**1a** to a zwitterionic hydrogenated product with a *gauche* conformation, *gauche*-PD**1**, is accompanied by an energy gain with respect to the reactants (*gauche*-**1** + H_2), and, at room temperature, the overall reaction is slightly exergonic (Figure 2A). The stabilization of *gauche*-PD**1** with respect to *gauche*-**1** + H_2 due to purely electronic factors notably diminishes upon consideration of entropic effects (cf. $\Delta E_{sol} \approx$ -32 kJ·mol^{-1} vs. $\Delta G_{sol} \approx$ -7

kJ·mol^{-1}). It is evident from Figure 2A, that the predicted energy profiles of the forward and backward reactions become very similar at room temperature, which is an indication for reversibility of the investigated reaction. To the best of our knowledge, however, the experimental findings published so far[2] have not identified the activation of H_2 by FLP**1** as a reversible process. Importantly, the crystal structure of the phosphonium-hydridoborate zwitterion $Mes_2PH^+CH_2CH_2BH^-(C_6F_5)_2$ isolated at the end of the reaction, is represented entirely by *trans* conformers, with PCCB torsion angle of about 180º and d_{PB} = 4.24 Å.[2] According to our calculations, the potential energy barrier required for the isomerization of *gauche*-PD**1** (with PCCB torsion angle of 311º) to *trans*-PD**1** (with PCCB torsion angle of 224º) is of the order of 29 kJ·mol^{-1}, which corresponds to essentially free rotation around the C–C axis of the molecule (Figure S2).[32] In the hydrogenated products (Figure 3A), the H–H bond is completely cleaved, as indicated by the large d_{HH} distance (2.17 Å in *gauche*-PD**1**, and 5.10 Å in *trans*-PD**1**), and the newly formed P–H and B–H bonds are of the same length in both conformations (d_{PH}=1.40 Å and d_{BH} = 1.23 Å). In comparison to TS**1a**, the phosphorus and boron sites in both *gauche*-PD**1** and *trans*-PD**1** are further polarized (Table 2) due to the attachment of H^+ at P, and H^- at B, as a consequence of the heterolytic splitting of H_2. Note that, according to the energy profile shown in Figure 2A, the *gauche*-PD**1** and *trans*-PD**1** products obtained via the *intramolecular* mechanism, are of essentially equal stability. The corresponding Boltzmann factor, calculated as $F_{trans\text{-PD}\mathbf{1}}/F_{gauche\text{-PD}\mathbf{1}} = \exp[(G_{gauche\text{-PD}\mathbf{1}}-G_{trans\text{-PD}\mathbf{1}})/RT]$, equals 1.1, which indicates that both conformations should be populated in equal amount at room temperature.[33] This appears to be in conflict with the earlier highlighted experimental fact that the structure of the phosphonium-hydridoborate salt of **1** consists of trans conformers only.[2] On the other hand, the conformation of the hydrogenated Lewis pair immediately after the reaction does not necessarily reflect the crystal structure, and hence, the presence of only *trans*-PD**1** conformers in the latter might be enforced by the crystal packing during the crystallization. Importantly, we have found that dimerization of *trans*-PD**1** is an exergonic process (see Figure 4 and related discussion), hence, it is likely that the hydrogenated product will adopt *trans* conformation upon crystal packing.

The key failure of the *intramolecular* concept was revealed, when we used it to rationalize the experimentally established[4] inability of the phenyl-substituted compound **2** (Table 1) to activate H_2. Assuming a reaction between the open *cis*-**2** conformer and H_2, we calculated the *intramolecular* reaction profile and, as Figure 2B shows, we found that the associated energy barriers are of similar height to those calculated for the *intramolecular* H_2 activation by FLP**1** (Figure 2A). In other words, the reaction of FLP**2** with H_2 should be as feasible as that of FLP**1** with H_2, however, such a prediction contradicts the experimental findings. Hence, the inertness of the phenyl-substituted FLP**2** cannot be explained by the concept for *intramolecular* H_2 activation.

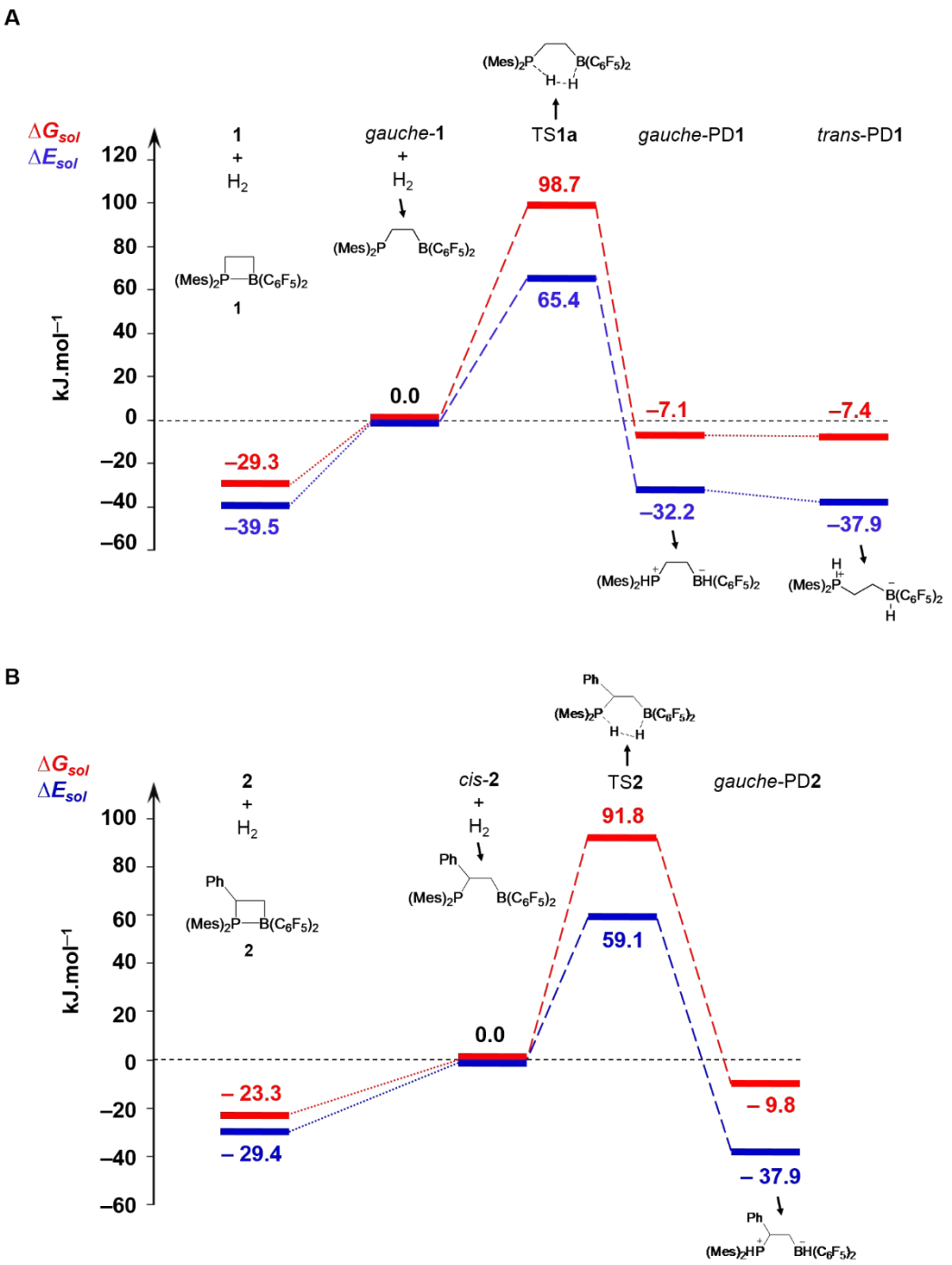

Figure 2. SCS–MP2/cc–pVTZ//B97D/6–31G(d) reaction profiles of an *intramolecular* H_2 activation driven by $Mes_2PCH_2CH_2B(C_6F_5)_2$, FLP**1**, in (A), and $Mes_2PCHPhCH_2B(C_6F_5)_2$, FLP**2**, in (B). The calculated solvent-phase Gibbs energies, ΔG_{sol}(298.15K), in red, and ZPE-corrected electronic energies, ΔE_{sol}(0K), in blue, are referred to the total energy of *gauche*-**1** and an isolated H_2 molecule (*gauche*-**1** + H_2) in (A), and to the total energy of *cis*-**2** and an isolated H_2 molecule (*cis*-**2** + H_2) in (B). The energetics of the non-reactive cyclic conformers **1** and **2** is shown only for completeness. The kinetic barrier, ΔE, associated to the *gauche*-*trans* isomerization of the product in (A), is shown in the Supporting Information. Used abbreviations: TS for transition state, and PD for hydrogenated product.

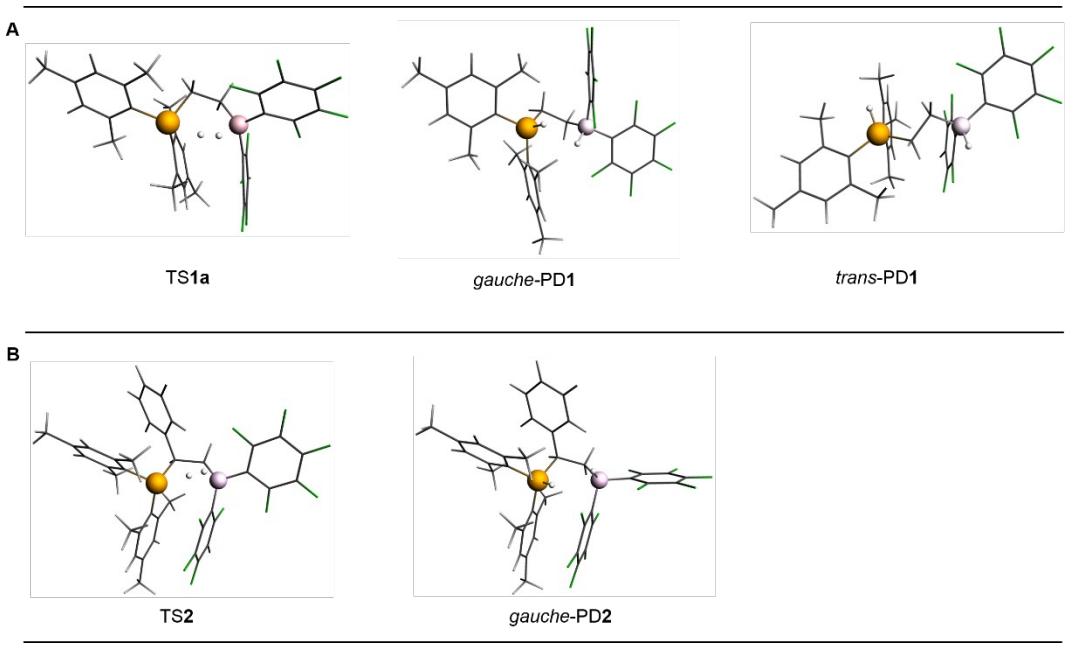

Figure 3. Fully-optimized (B97D/6–31G(d)) structures of the stationary points along the reaction coordinate of an *intramolecular* H_2 activation by $Mes_2PCH_2CH_2B(C_6F_5)_2$, FLP**1**, in (A), and $Mes_2PCHPhCH_2B(C_6F_5)_2$, FLP**2**, in (B) (see also Scheme 1 and Figure 2). For the structures of the initial reactants, namely, *gauche*-**1** and *cis*-**2**, see Figure 1. Color code: P yellow, B pink, F green, C grey, H white. Used abbreviations: TS for transition state and PD for hydrogenated product.

***Intermolecular* H_2 activation.** To cope with the issues faced by the *intramolecular* concept, we searched for a different reaction mechanism, and for FLP**1**, we found an alternative, *intermolecular* channel, which is illustrated in Figure 4 (see also Scheme 2). Within this mechanism, the *gauche*-*trans* isomerization, which, as highlighted above, turns to be rather feasible (with an estimated kinetic barrier of ~30 kJ·mol^{-1}), is assumed to take place before the reaction with H_2. Moreover, the *trans*-**1** conformer was found to be slightly more stable than the *gauche*-**1** conformer (ΔG_{sol} and ΔE_{sol} of about 15 kJ·mol^{-1}, Figure 4). Though the distance between the Lewis sites in *trans*-**1** (d_{PB} = 4.04 Å) is large enough for accommodating H_2, some structural features, such as the arrangement of P and B on opposite sides of the C–C bridge, and the presence of π–stacked Mes and C_6F_5 substituents (see Figure 1A), preclude the formation of a properly arranged *trans*-**1**···H_2 intermediate that can ensure sufficient interaction between *trans*-**1** and H_2 for subsequent H_2 splitting. In view of this, we considered the possibility of having a dimer of *trans* monomers to be responsible for the reaction with hydrogen. As shown in Figure 4, the dimerization of two *trans*-**1** to dimer-**1** is favored on electronic grounds ($\Delta E_{sol} \approx 67$ kJ·mol^{-1}),[34] but when thermal contributions are accounted for, the stabilization of the dimer with respect to the monomer becomes negligible (ΔG_{sol} = 1.3 kJ·mol^{-1}).[35,36] In the structure of dimer-**1**, the phosphorus and boron belonging to one and the same *trans* monomer become slightly more distant from each other (d_{PB} = 4.11 and 4.16 Å), as compared to the situation in the monomeric *trans*-**1**. Most importantly, the structure of dimer-**1** (Figure 5) provides an optimum arrangement of the Lewis sites belonging to different monomers. The P and B sites of one monomer are well exposed to the B' and P' sites, respectively, of the other monomer, and the

intermolecular distances, $d_{PB'}$ = 3.81 Å and $d_{P'B}$ = 4.51 Å, fall in the optimum range[13] for triggering a cooperative acid-base action of the oppositely lying Lewis centers, what will eventually cause polarization and cleavage of the H–H bond. In this respect, dimer-**1** resembles a typical *intermolecular* FLP which, instead of only one, provides two regions prone to react with H_2.[35] As shown in Figure 5, dimer-**1** is stabilized by non-covalent interactions between the aromatic groups in the *trans*-**1** monomers: each C_6F_5 ring at boron arranges in a parallel-displaced conformation with the nearest Mes substituent at phosphorus. Upon the attack of a hydrogen molecule the system reorganizes into a TS**1b** state at an energy cost (ΔE_{sol}) of about 54 kJ·mol^{-1}, with respect to isolated dimer-**1** and H_2. As in the case of the *intramolecular* mechanism (Figure 2A), the consideration of thermal effects increases this activation barrier by 30 kJ·mol^{-1} ($\Delta G_{sol} \approx$ 84 kJ·mol^{-1}, relative to dimer-**1** + H_2), see Figure 4. Alike in TS**1a**, H_2 locates away from the P–B' axis, in a non-parallel fashion (PHH = 176º and B'HH = 106º), see Figure 5. The single imaginary frequency (f_i = -110 cm^{-1}) of TS**1b** corresponds to the H–H stretching and the motion of H_2 towards phosphorus and boron framing one of the two *intermolecular* active sites. The H–H bond stretches to 0.80 Å, while the partially formed P–H and B–H bonds are respectively by ~0.2 and ~0.1 Å longer than those in TS**1a**. The entrapment of a single H_2 in TS**1b** affects the intermolecular P−B distances ($d_{PB'}$ and $d_{P'B}$), which differ by more than 2 Å from each other (Table 2), as well as the orientation of the aryl substituents (Figure 5). While at the site of the H_2 attack, P and B' lie in close proximity ($d_{PB'}$ = 3.72Å), and the C_6F_5 and Mes groups retain almost the same configuration as in the dimer-**1** reactant, at the non-hydrogenated site, P' and B move away from each other ($d_{P'B}$ = 5.78 Å), and the π-stacking between the substituents is lost. The partial charge distribution over the P···H···H···B' bridge in TS**1b** resembles that in TS**1a**, whereas the atomic charges of the non-hydrogenated P' and B are similar to those in the *trans*-**1** monomer (Table 2). Relaxation of TS**1b** in the forward direction yields the monohydrogenated product, dimer-PD**1**, which at room temperature (ΔG_{sol}) turns to be by 37 kJ·mol^{-1} less stable than the isolated reactants, dimer-**1** + 2H_2 (Figure 4). The P–H and B'–H bonds in dimer-PD**1** are of typical length, and the polarization of the hydrogenated Lewis sites is the same as in the *trans*-PD**1** product of the *intramolecular* mechanism (cf. values in Table 2). In the same time, the polarization of the cleaved hydrogen molecule is stronger than in *trans*-PD**1**, and can be attributed to the much shorter distance between the proton and the hydride (cf. d_{HH} = 1.94 Å in dimer-PD**1** vs. 5.10 Å in *trans*-PD**1**). Importantly, the distance between the non-hydrogenated Lewis sites in dimer-PD**1** ($d_{P'B}$ = 4.48 Å), as well as the associated partial charges (Table 2), are suitable for preconditioning uptake of a second H_2 molecule.[37] As indicated by the energy profiles in Figure 4, the activation barrier for hydrogenation of dimer-PD**1** is of the order of 72 kJ·mol^{-1} at room temperature (and ~35 kJ·mol^{-1} at 0K), that is slightly less than the activation barrier of the first hydrogenation reaction. The final step within the *intermolecular* mechanism is the relaxation of TS**1c** (with f_i = -115 cm^{-1}) to the dihydrogenated product, dimer-PD**1'**, which is found to be more stable than the monohydrogenated dimer-PD**1** ($\Delta G_{sol} \approx$ 40 kJ·mol^{-1}, $\Delta E_{sol} \approx$ 77 kJ·mol^{-1}). As shown in Figure 5, the structure of dimer-PD**1'** consists of two hydrogenated *trans* monomers held in

proximity ($d_{PB'}$ = 3.90 Å, and $d_{P'B}$ = 4.37 Å) by the π-stacked aryl substituents, and the electrostatic interaction between the zwitterionic monomers. In this final product, the two H_2 molecules are heterolytically cleaved, as evidenced by its structural features (H···H distances, P–H and B–H bond lengths), and the charge distribution over the two P–H···H–B fragments, see Table 2. Worth noting is that in the reported crystal structure of the phosphonium-hydridoborate salt of **1**,[2] one can find similar (yet, not exactly the same) stacking of the respective *trans* conformers, with the shortest P···B' (and P'···B) contacts of 4.09 Å. Importantly, as Figure 4 shows, the overall reaction within the *intermolecular* mechanism, that is 2*gauche*-**1** + $2H_2$ → dimer-PD**1'**, is exergonic (ΔG_{sol} = -33 kJ·mol^{-1}), which, unlike the energetics of the *intramolecular* mechanism (Figure 2A), conforms well with the experimental result for a non-reversible (at room temperature) H_2 activation by FLP**1**. Another advantage of the *intermolecular* over the *intramolecular* reaction channel is that the associated maximum activation barrier is by almost 20 kJ·mol^{-1} lower for the former as compared to the latter mechanism (cf. energies of TS**1c** and TS**1a** in Figures 4 and 2A, respectively).

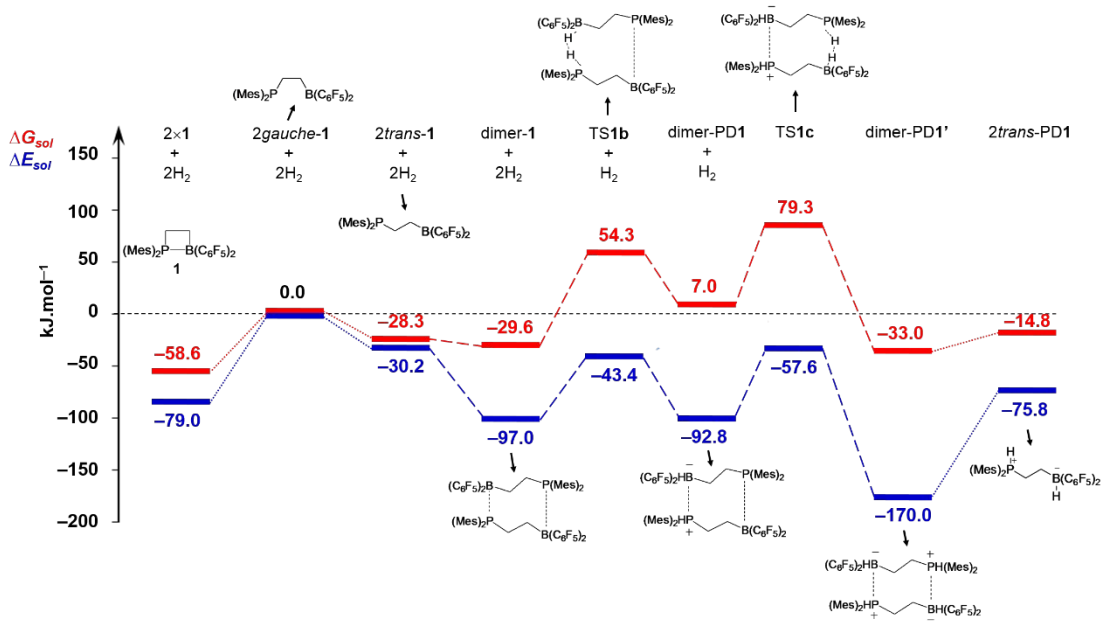

Figure 4. SCS–MP2/cc–pVTZ//B97D/6–31G(d) reaction profile of an *intermolecular* H_2 activation driven by $Mes_2PCH_2CH_2B(C_6F_5)_2$, FLP**1**. The calculated solvent-phase Gibbs energies, ΔG_{sol}(298.15K), in red, and ZPE-corrected electronic energies, ΔE_{sol}(0K), in blue, are referred to the total energy of two isolated *gauche*-**1** conformers and two isolated H_2 molecules (2*gauche*-**1** + $2H_2$). The energetics of the non-reactive cyclic conformer **1**, and the monomeric product *trans*-PD**1** are shown only for completeness. The kinetic barrier, ΔE, associated to the *gauche-trans* isomerization of the reactant is shown in the Supporting Information. Used abbreviations: TS for transition state, and PD for hydrogenated product.

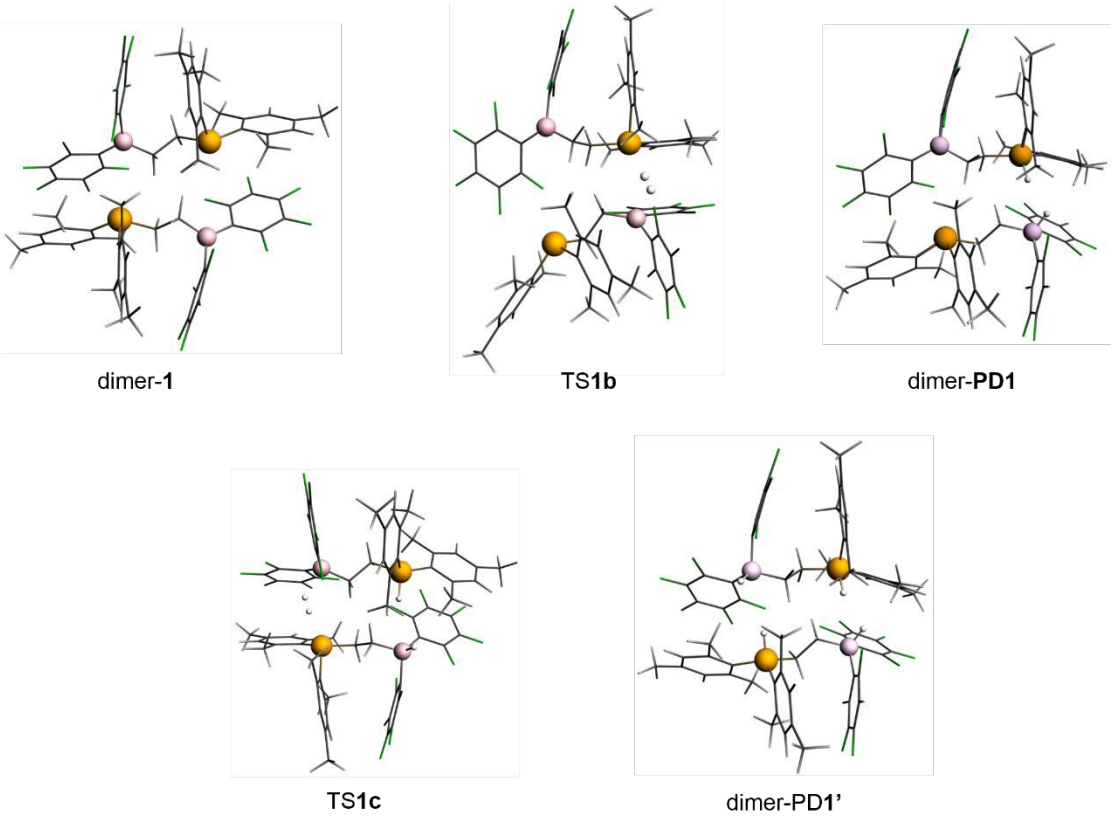

Figure 5. Fully-optimized (B97D/6–31G(d)) structures of the stationary points along the reaction coordinate of an *intermolecular* H_2 activation by $Mes_2PCH_2CH_2B(C_6F_5)_2$, FLP**1** (see also Scheme 2 and Figure 4). For the structure of the initial reactant, *trans*-**1**, see Figure 1A. Color code: P yellow, B pink, F green, C grey, H white. Used abbreviations: TS for transition state and PD for hydrogenated product.

If we apply the *intermolecular* concept to the phenyl-substituted FLP**2** (Table 1), we have to consider formation of weakly-bound dimers of *trans*-**2** monomers (Figure 2B), for ensuring closely lying and exposed to each other P and B sites. However, in the predicted structure of such a dimeric assembly (Figure S3), the *intermolecular* distance between the Lewis sites ($d_{PB'}$, $d_{P'B}$) is almost 6 Å, which, as shown earlier,[13] is way too large to precondition reaction with H_2. Due to the increased steric hindrance caused by the additional phenyl substituent at the C–C bridge in the molecule, the individual *trans*-**2** conformers stay apart, thus, the Lewis sites remain too distant from each other, and are unable to promote polarization of H_2, and subsequent cleavage of the H−H bond. Hence, the *intermolecular* concept provides a rationale for the inertness of FLP**2** with respect to H_2, in agreement with the published experimental findings.[4] Moreover, the different activity of the other two substituted derivatives of **1** can be understood on the same grounds: The bulky $SiMe_3$ group in FLP**3** hampers the dimerization of the open-chain conformers, and also blocks the boron acidic site (Figure S4a in the Supporting Information), which in turn, inhibits the activity of **3**. In contrast, the relatively small methyl substituent in **4** renders the system less hindered and more flexible, hence, its non-cyclic *trans* conformers (Figure S4b) can combine into weakly-bound dimers (Figure S5) allowing for an *intermolecular* activation of H_2. Thus, we can conclude that the steric hindrance imposed by the substituents at the C–C bridge in the structure of linked FLPs of the type studied

here plays a primary role for the activity of such systems towards molecular hydrogen.

Table 2. Selected distances and bond lengths (in Å), and natural charges (in units of elementary charge) of the P, B and H atoms from H_2, as obtained for the stationary points along the reaction paths of the *intramolecular* and *intermolecular* mechanisms of the H_2 activation by FLP**1**. TS and PD denote transition state and hydrogenated product, respectively. H_P and H_B denote the hydrogen atoms that are close or bound to phosphorus and boron, respectively. The equilibrium H−H bond is calculated as d_{HH} = 0.74 Å. All parameters are derived from B97D/6-31G(d) calculations in gas phase.

Stationary points along the reaction coordinate	**Distances and bond lengths**				**Natural charges**			
	d_{PB}, Å	d_{PH}, Å	d_{BH}, Å	d_{HH}, Å	P	B	H_P	H_B
			Intramolecular mechanism					
1	2.25 [a]	—	—	—	1.16	0.42	—	—
gauche-**1** + H_2	3.28 [a]	—	—	—	0.83	0.85	0.00	0.00
TS**1a**	3.36 [a]	1.93	1.55	0.83	0.92	0.58	+0.12e	-0.01
gauche-PD**1**	3.16 [a]	1.40	1.23	2.17	1.34	0.12	0.06	-0.03
trans-PD**1**	4.07 [a]	1.40	1.22	5.10	1.33	0.14	0.04	0.00
			Intermolecular mechanism					
trans-**1** + H_2	4.04 [a]	—	—	—	0.85	0.85	0.00	0.00
dimer-**1** + H2	3.81/4.51 [b]	—	—	—	0.83/0.81	0.92/0.92	0.00/—	0.00/—
TS**1b**	3.72/5.78 [b]	2.13/—	1.64/—	0.80/—	0.92/0.83	0.65/0.86	0.12/—	0.00/—
dimer-PD**1**	3.87/4.48 [b]	1.40/—	1.24/—	1.94/—	1.35/0.80	0.16/0.91	0.07/—	-0.05/—
TS**1c**	4.16/4.14 [b]	1.40/2.24	1.23/190	2.62/0.79	1.34/0.88	0.14/0.75	0.06/0.08	-0.02/-0.05
dimer-PD**1'**	3.90/4.37 [b]	1.40/1.40	1.23/1.23	2.18/2.89	1.33/1.35	0.16/0.14	0.05/0.04	-0.03/-0.01

[a] The tabulated values for d_{PB} correspond to *intramolecular* P−B distances; [b] The tabulated values for d_{PB} correspond to *intermolecular* P−B distances.

Conclusion

Using quantum-chemical calculations, we have examined two different concepts for the mechanism of H_2 activation by linked FLPs of the type $Mes_2PCHRCH_2B(C_6F_5)_2$, with R = H (in FLP**1**), Ph (in FLP**2**), $SiMe_3$ (in FLP**3**) or Me (in FLP**4**), in order to explain the unusual behavior of these systems in the presence of molecular hydrogen. The two concepts assume that different initial state of the FLP is responsible for the reaction with H_2. We have shown that the *intramolecular* concept known from the literature,[10,12] which assumes a bimolecular concerted reaction between an open-chain *gauche* FLP conformer and one hydrogen molecule, can not explain the experimentally established[4] inertness of FLP**2** towards H_2. We have rationalized this experimental fact by proposing an alternative, *intermolecular* reaction mechanism, that requires stacking of two open-chain *trans* FLP

conformers into a dimer-like reactant resembling an *intermolecular* FLP with two reactive pockets, which can activate up to two hydrogen molecules. Within the *intermolecular* reaction channel, the formation of *gauche* FLP···H_2 intermediates is avoided, thus only *trans* conformers of the zwitterionic salts are obtained at the end of the reaction, which is consistent with the experimental result for FLP**1**. Furthermore, in the presence of a bulky substituent like Ph (in FLP**2**) or $SiMe_3$ (in FLP**3**), the *intermolecular* channel becomes inaccessible due to the imposed extra steric hindrance around the Lewis sites, which prevents the dimerization of the open-chain FLP conformers into weakly-bound intermediates that can react with H_2. This characteristics of the *intramolecular* mechanism is the limiting factor that explains the experimentally established inertness of the phenyl- and trimethylsilyl- substituted FLPs. Overall, our findings suggest that the activity of the *intramolecular* (linked) FLPs towards heterolytic splitting of H_2 is actually of *intermolecular* character, which in turn highlights the importance of steric factors and noncovalent interactions for the design of metal-free systems that can cleave the H−H bond, and serve as hydrogenation catalysts. Our calculations suggest additional experimental investigations to elucidate the H_2 activation in these compounds, most importantly concentration-dependent studies that should allow the identification of the correct reaction mechanism.

Acknowledgements

L. L. Z., P. St. P. and N. V. thank Dr. Maxim Ponomarenko for helpful discussions. Financial support by Solvay Fluor GmbH is gratefully acknowledged.

References

1. G. C. Welch, R. R. San Juan, J. D. Masuda and D. W. Stephan, *Science*, 2006, **314**, 1124–1126.
2. P. Spies, G. Erker, G. Kehr, K. Bergander, R. Fröhlich, S. Grimme and D. W. Stephan, *Chem. Commun.*, 2007, **2**, 5072–5074.
3. D. W. Stephan, *Org. Biomol. Chem.*, 2008, **6**, 1535–1539.
4. P. Spies, G. Kehr, K. Bergander, B. Wibbeling, R. Fröhlich and G. Erker, *Dalt. Trans.*, 2009, **38**, 1534–1541.
5. D. W. Stephan and G. Erker, *Angew. Chem. Int. Ed. Engl.*, 2010, **49**, 46–76.
6. F.-G. Fontaine, M.-A. Courtemanche and M.-A. Légaré, *Chem. Eur. J.*, 2014, **20**, 2990–2996.
7. Y. Guo and S. Li, *Inorg. Chem.*, 2008, **47**, 6212–6219.
8. T. A. Rokob, A. Hamza, A. Stirling, T. Soós and I. Pápai, *Angew. Chem. Int. Ed. Engl.*, 2008, **47**, 2435–2438.
9. T. A. Rokob, A. Hamza and I. Papai, *J. Am. Chem. Soc.*, 2009, **131**, 10701–10710.
10. S. Grimme, H. Kruse, L. Goerigk and G. Erker, *Angew. Chemie Int. Ed.*, 2010, **49**, 1402–1405.
11. M. Pu and T. Privalov, *J. Chem. Phys.*, 2013, **138**, 154305.
12. T. A. Rokob, I. Bakó, A. Stirling, A. Hamza and I. Pápai, *J. Am. Chem. Soc.*, 2013, **135**, 4425–4437.

13. L. L. Zeonjuk, N. Vankova, A. Mavrandonakis, T. Heine, G.-V. Röschenthaler and J. Eicher, *Chem. Eur. J.*, 2013, **19**, 17413–17424.

14. M. J. Frisch, G. W. Trucks, H. B. Schlegel, G. E. Scuseria, M. A. Robb, J. R. Cheeseman, G. Scalmani, V. Barone, B. Mennucci, G. A. Petersson, H. Nakatsuji, M. Caricato, X. Li, H. P. Hratchian, A. F. Izmaylov, J. Bloino, G. Zhe, and D. J. F. Gaussian 09, Revision D.01.

15. R. Ahlrichs, M. Bar, H. P. Baron, R. Bauernschmitt, S. Bocker, M. Ehrig, K. Eichkorn, S. Elliot, F. Furche, M. Haser, H. Horn, C. Hattig, C. Huber, U. Huniar, M. Kattanneck, A. Kohn, C. Kolmel, M. Kollwitz, K. May, C. Ochsenfeld, H. Öhm, A. Schafer, U. Sc, H. W. TURBOMOLE 5.9.1, Universität Karlsruhe, 2007.

16. S. Grimme, *J. Comput. Chem.*, 2006, **27**, 1787–1799.

17. G. a. Petersson, A. Bennett, T. G. Tensfeldt, M. a. Al-Laham, W. a. Shirley and J. Mantzaris, *J. Chem. Phys.*, 1988, **89**, 2193–2218.

18. G. a. Petersson and M. a. Al-Laham, *J. Chem. Phys.*, 1991, **94**, 6081–6090.

19. R. February, *Acc. Chem. Res.*, 1981, **14**, 363–368.

20. J. P. Foster and F. Weinhold, *J. Am. Chem. Soc.*, 1980, **102**, 7211–7218.

21. J. Tomasi, B. Mennucci and R. Cammi, *Chem. Rev.*, 2005, **105**, 2999–3093.

22. S. Grimme, *J. Chem. Phys.*, 2003, **118**, 9095–9102.

23. T. H. Dunning, *J. Chem. Phys.*, 1989, **90**, 1007–1023.

24. F. Weigend and M. Haser, *Theor. Chem. Acc.*, 1997, **97**, 331–340.

25. M. Feyereisen, G. Fitzgerald and A. Komomicki, *Chem. Phys. Lett.*, 1993, **208**, 359–363.

26. J.-D. Chai and M. Head-Gordon, *Phys. Chem. Chem. Phys.*, 2008, **10**, 6615–6620.

27. R. Ditchfield, *J. Chem. Phys.*, 1971, **54**, 724.

28. M. J. Frisch, J. a. Pople and J. S. Binkley, *J. Chem. Phys.*, 1984, **80**, 3265.

29. T. Clark, J. Chandrasekhar, G. W. Spitznagel and P. V. R. Schleyer, *J. Comput. Chem.*, 1983, **4**, 294–301.

30 S. Grimme, J. Antony, S. Ehrlich and H. Krieg, *J. Chem. Phys.*, 2010, **132**, 154104.

31 Y. Zhao and D. G. Truhlar, *Theor. Chem. Acc.*, 2007, **120**, 215–241.

32. To estimate the energy barrier for the *gauche-trans* isomerization, we did a relaxed PES scan with respect to the PCCB torsion angle (the details are given in the Supporting Information).

33. As shown in Figure 2A, even at 0K, the calculated energy difference between *gauche*-PD**1** and *trans*-PD**1** is less than 6 kJ•mol^{-1}.

34. The dimerization energy of the *trans* conformers of **1** to dimer-like species is subjected to basis set superposition error (BSSE). We have estimated the counterpoise correction (CP) to be of the order of 50 kJ•mol-1 (details in Table S9, but as pointed out in previous studies, such a value is probably overestimated due to basis set incompleteness. For details, see: J. Antony, S. Grimme, *J. Phys. Chem. A* 2007, **111**, 4862–4868, and T. A. Rokob, A. Hamza, A. Stirling, T. Soos, I. Pápai, *Angew. Chem.* 2008, **120**, 2469–2472; *Angew. Chem. Int. Ed.* 2008, **47**, 2435–2438.

35. Neither dimer-like assemblies, nor open-chain (*gauche* and/or *trans*) conformers have been found in the experimental solution of **1** (P. Spies, G.Erker, G. Kehr, K. Bergander, R. Fröhlich, S. Grimme, D. W. Stephan, *Chem. Commun.* 2007, **2**, 5072–5074). This is similar to the situation in the case of intermolecular (non-linked) FLPs, for which only the individual Lewis components are typically detected in the respective stoichiometric mixtures at ambient conditions (G. C. Welch, D. W. Stephan, *J. Am. Chem. Soc.* 2007, **129**, 1880–1881). Most probably, these are species of a short lifetime, and therefore, could not be detected in the time-frame of the NMR measurements, that are commonly employed for characterizing the FLPs' solution structure.

36. In reality, the ratio between *trans*-**1** and its dimeric assembly dimer-**1** is expected to be strongly dependent on the concentration of the reaction solution of **1**. We note that this is not taken into account in the discussed calculations. Furthermore, we note that the energy barriers in terms of both ΔE_{sol} and ΔG_{sol}, calculated for weakly interacting systems as those studied here, are subjected to non-negligible errors due to certain limitations of the computational approach: the values of ΔE_{sol} are most probably overestimated due to BSSE, whereas the values of ΔG_{sol} are most probably underestimated due to the use of the rigid-rotor harmonic approximation. In this respect, the ΔE_{sol} and ΔG_{sol} energy profiles in Figure 4 map respectively the lowest and the highest borderline, while the "true" energy profile is to lie somewhere in-between.

37. In reality, the dimer-**1** reactant (Figure 4) can be attacked by two H_2 molecules simultaneously. The employed computational procedure, however, allows us to model the reaction with two H_2 molecules as consisting of two successive steps.